Asian Journal of Information Technology 15 (24): 5084-5092, 2016
ISSN: 1682-3915

A Semi-Automatic Segmentation Approach for Kidney Stone Detection in Ultrasound Images

T. Loganayagi
Department of Electronics and Communication Engineering, Selvam College of Technology, Namakkal, Tamil Nadu, India

Abstract: Ultrasound imaging is a non-invasive and inexpensive technique for detection of kidney stones. As the ultrasound images are affected by speckle noise, the segmentation of the images remains a challenging task. The manual detection and measurement of segmented stones become cumbersome and suffers from inter-observer variability. Hence, a computer aided algorithm is required for automatic stone detection and reproducibility with robust despeckling and segmentation techniques. In this study, an algorithm is developed by using Adaptive Bilateral Filter (ABF) for reducing speckle noise and mathematical morphological operations for segmentation of stones in ultrasound kidney images. The speckle reduction performance of ABF is evaluated byPeak Signal to Noise Ratio (PSNR), Structural Similarity Index Metrics (SSIM) and Edge Preservation Index (β).The proposed stone detection algorithm is analyzed through Pratt's Figure of Merit (FOM).

Key words: Ultrasound images, kidney stone, adaptive bilateral filter, sobel edge detection, morphological operation

INTRODUCTION

The prevalence of kidney stone is a most common problem in human urinary system (Fwu *et al*., 2013; Moe, 2006; Rafiei *et al*., 2014; Romero *et al*., 2010; Zayid *et al*., 2014). Kidney stones consist of various organic and inorganic substances such as calcareous, uric acid, cysteine, struvite and ammonium acid combined with proteins (Moe, 2006). The kidney stones can be inferred with various pathophysiological symptoms like lumbar discomfort and dysuria. Conversely certain non-calcareous stones have singular pathophysiology whichis not adequate for any diagnostic and therapeutic efforts. However, due to less common physiological symptoms, the clinicians depend on various medical imaging procedures like sonogram, radiograph or Computed Tomography (CT). The use of CT in kidney stone detection provides accurate diagnostic information (Fwu *et al*., 2013; Khan *et al*., 2004). But the repeated use of CT diagnostic for patient with renal calculi contributes to an increased exposure of radiation (Fwu *et al*., 2013). B-mode ultrasound is the best medical imaging technique compared to CT, (Magnetic Resonance Imaging) MRI, etc., concerning their ability of providing good anatomical details of kidney in a short period, absence of radiation, no usage of contrast agent, safe to obstetric patients and low-cost (Khan *et al*., 2004). However, the visualization of ultrasound images is affected by speckle noise. The characterization of speckle is a bright non-calculus echo present in ultrasound images which mimics as renal calculi (Khan *et al*., 2004). The ultrasound stone images are mainly characterized by its large reflectivity. If the size of the stone is dense and large, the echo beam intensity will be higher and the stone looks brighter than the surrounding tissues. The sensitivity of ultrasound imaging is higher (nearly 100%) in detection of large and dense calculi. The challenge for ultrasound imaging is the detection of smaller non shadow calculi.

Mitterberger *et al*. (2009) addressed the kidney stone detection problems in ultrasound image usinga comparative analysis with Doppler ultrasound. This analysis is helped in this work to understand twinkling artifacts caused by the speckle noise. Nirali *et al*. (2014) discussed thespeckle filtering and enhancement techniques to improve the image quality and their performances. This information was advantageous in understanding the existing filtering and enhancement techniques. Tomasi and Manduchi (1998) proposed an edge preserving, non-iterative Bilateral Filter (BF) for gray and color image with additive Gaussian noise. This filter property was essential in case of medical ultrasound images. Bhonsle *et al*. (2012) utilized the Bilateral filter for various medical images including X-ray, MRI, CT and ultrasound considering the smoothing of Gaussian noise. It was proved that the performance of bilateral filter is better than the linear filters and removes the noise in the high frequency areas. For the better reduction of speckle noise, Bhonsle *et al.* (2012) suggested to convert the multiplicative speckle model into an additive model.

Tang *et al.* (2010) offered an ABF concept for speckle noise reduction in ultrasound cattle follicle images.In their research, ABFwas derived from the multiplicative noise model instead of additive model used in bilateral filter (Tomasi and Manduchi, 1998). The ABF performance was better than the bilateral filter by improving the contrast value and edge preservation in homogeneous regions. Tamilselvi and Thangaraj (2011ab, 2010, 2012); Tamilselvi (2013) presented and tested various automatic and semi-automatic segmentation algorithms such as Artificial Neuro Fuzzy Inference System (ANFIS) system, active contour, watershed segmentation, morphology, thresholding and K-means clustering over ultrasound renal images to detect calculi. The analysis of Tamilselvi and Thangaraj (2011a, b, 2010, 2012) and Tamilselvi (2013) helped to select a segmentation technique for kidney stones. Kop and Hegadi (2010) had proposed gradient vector flow segmentation and Sridhar (2012) proposed a region growing segmentation for ureteric and bladder calculi detection in ultrasound images.These techniques require seed point and initial contour selection for segmentation which was not comfortable for the physicians during computer aided segmentation process. Hafizah and Supriyanto (2012, 2010) and Hafizah *et al.* (2012) discussed the morphological based region of interest generation and segmentation along with various filtering and texture analysis procedure for ultrasound kidney images. The Hafizah *et al* (2010) research helpedto understand that the morphological operation on ultrasound image provides proper texture extraction. The computer aided semi-automatic segmentation wasachieved effectively by the morphological segmentation.

Balocco *et al.* (2010) proposed the Speckle Reducing Bilateral Filter (SRBF) for ultrasound images. SRBF was the extension of bilateral filter framework by calculating thefilter coefficients using Rayleigh PDF and autocorrelation matrix of the noisycoefficient. Raj and Veukateswarlu (2012) and Wan and supriyanto (2010) applied the BF filter framework on wavelet coefficients of ultrasound images to eliminate the noise.The concept of this multi-resolution approach is to distinguish the noiseand image information at each level of decomposition.

Sandhiyakumari *et al.* (2008, 2011) developed a medical decision making system for ultrasound carotid artery indiagnosis and classification.These works were useful in comprehending theconcept of automatic diagnosis of ultrasound images. Gupta *et al.* (2010). presented an automatic detection of kidney stones with two algorithms and they made comparison of both. The robustness of both the algorithms based on efficiency and relative error in stone area. Even though the algorithmic performance was high with reduced error rate, the edge preservation was weak when using Speckle Reducing Anisotropic Diffusion (SRAD) filter. In this study an attempt is made for speckle reduction in ultrasound images that facilitate a better segmentation of kidney stone.

MATERIALS AND METHODS

Image filtering: Gupta *et al.* (2010) utilized a Speckle Reducing Anisotropic Diffusion (SRAD) Filtering for speckle reduction followed by unsharp filtering. The author mentioned that the SARD islow in edge preservation and showing salt and pepper noise in the filtered image. This hampers the segmentation process and needs an image sharpening using unsharp filter. The histogram equalization is also required to improve the brightness of the stone. To preserve the edges, this study uses ABF used for pre-processing. The ABF developed for US image in cattle follicle segmentation by Tang *et al.* (2010) is used here for kidney image enhancement which is given as:

$$\tilde{F}(X) = \frac{1}{C}\sum Y \in N(X) \times \frac{-\|y-x\|^2}{2\sigma^2 d}\, e^{-\frac{-|F(Y)-FX|^2}{2\|F(X)\|^2\sigma^2 r}}\, F(Y) \tag{1}$$

Where:

$$C = \sum Y \in N(X) e^{\frac{-(x^2+y^2)}{2\sigma^2 d}} \times e^{-\frac{-|F(Y)-F(X)|^2}{2\|F(X)\|^2\sigma^2 r}} \tag{2}$$

Equation 1 is an adaptive bilateral filter for image with speckle noise where, X and Y are the spatial distance between a pixel and its neighborhood in the given window. |F(Y)-F(X)| measures the distance between the two intensity values of pixels X and Y. The first term in Eq. 1 relates to the low pass Gaussian domain filter which measures the closeness of geometric distance between two pixels where the second term corresponds to low pass range filter which measures the photometric similarity between F(Y) and (X).The normalization factor C in Eq. 1 ensures that the weight for all the pixels add up to one. The σ_d is the geometric spread parameter in domain filtering and σ_r is the photometric spread parameter in range filtering. The σ_d value indicates the amount of low pass filtering whereas σ_r determines the amount of range filtering required. More specifically, scaling an image up or down is done by adjusting σ_d and amplified or attenuated by adjusting σ_r. The experimental outcomes confirm that the ABF performance depends on the parameters such as window size w and standard deviations σ_d ,σ_r.

Morphological segmentation: The objects having structural and topological properties use the mathematical morphology concept for its segmentation. The dilation and erosion are the two basic operations performed in mathematical morphology followed by gradient, opening, closing and segmentation.The dilation operation allows the structuring element of the original object to grow larger. The erosion operation deletes the pixel in the dilated image matches the structuring element.

There are two basic ideas in morphological segmentation that include; finding contour of the object reconstruction of object of interest by assembling similar points. The contour of the object is resolved by main morphological tool known as watershed operator. The object segmentation uses feature extraction by operating various shape structuring elements. There two types of morphologies used are Gray scale morphology and Binary morphology.The basic operations are given in the below Eq. 3 and 4:

$$(f \oplus s)(x,y) = \max\{f(x-a, y-b)+s(a,b)\} \quad (3)$$

$$(f \ominus s)(x,y) = \max\{f(x-a, y-b)-s(a,b)\} \quad (4)$$

Where:

f = The original gray scale or binary image
s = Structuring element operated on f(x,y) is the pixel of an image f
a,b = The size of structuring element s

After morphological operations the required shape of object, edges, holes, corners and cracks can be extracted. The edge detection process utilizes the abrupt intensity change among the pixels of the background image and region of interest. In a noisy image, the edge is a set of connected noisy and noise free pixels. This may cause false edges and leads to misinterpretation of medical images. Hence in this study ABF Shi *et al*. (2010) is used to attenuate the amplitude of the noisy pixel and to preserve the actual edges. After applying ABF, the consideration of Sobel operator along with morphological operations detects the region of interest effectively.

Proposed kidney stone detection algorithm: In this study an improved combined method is proposed to segment the stone(s) in the ultrasound kidney images. The edge preserving ABF is applied on speckled ultrasound renal image to despeckle it. The gradient mask of the despeckled image is obtained using the Sobel operator. The gradient mask contains gaps which are not quite describing the outline of the calculi region. In order to fill the gaps in gradient binary mask, the morphological dilation and erosion operations are applied on the gradient mask to smooth the image by filling the inner gaps and to find the outline of the calculi region. Fig.1 shows the flow graph of the proposed method.

Voluson E-8 expert professional diagnostic ultrasound system (developed and produced by GE health care)is used for data acquisition of kidney images. It uses high resolution scanner with curved array transducer with a frequency range of 5-7.5 MHz. The acquired images are stored in computer as JPEG or BMP format for further processing. The image digitization step is performed to implement the proposed algorithm. The filtering is the next step to get the better quality of images with initial setting of filter parameters such as window size (w), domain filter parameter σ_d and range filter parameter σ_r. The filtered image quality is analyzed using PSNR and SSIM metrics before segmentation. The filtered images possess high quality when its SSIM value close to 1. If the image quality is not in acceptable, the σ_d and/(or) σ_r values are adjusted to get the required quality. The Sobel operation is performed over the filtered image to obtain binary mask. Then, the morphological operation is done in order to segment and mark the outline of the stone edges. Finally, the stone area is measured either manually or automatically by marking the required segmented portion. The proposed algorithm is implemented using MATLAB image processing tool box.

Performance assessment: The proposed algorithm is evaluated in two ways Eq. 1 the performance of ABF investigated using PSNR, SSIM and edge preservation index (β) Eq. 2 the morphological edge detection performance is analyzed in terms of Pratt Figure of Merit (FOM) and calculi area measurement. PSNR measures noise reduction between the two images under consideration and is given by:

$$\text{PSNR} = 20\log_{10}\frac{255}{\text{RMSE}}\text{dB} \quad (5)$$

The SSIM is another image quality metric which is correlated to the visual perception of human sensory system of vision. SSIM can be exploited as a benchmark to measure the image quality, thereby checking the performance of various image processing algorithms.

$$\text{SSIM}(f,F) = \frac{(2\mu_f\mu_F + C_1)\times(2\mu_{fF} + C_2)}{(\mu_{f^2} + \mu_{F^2} + C_1)\times(\mu_{f^2} + \mu_{F^2} + C_2)} \quad (6)$$

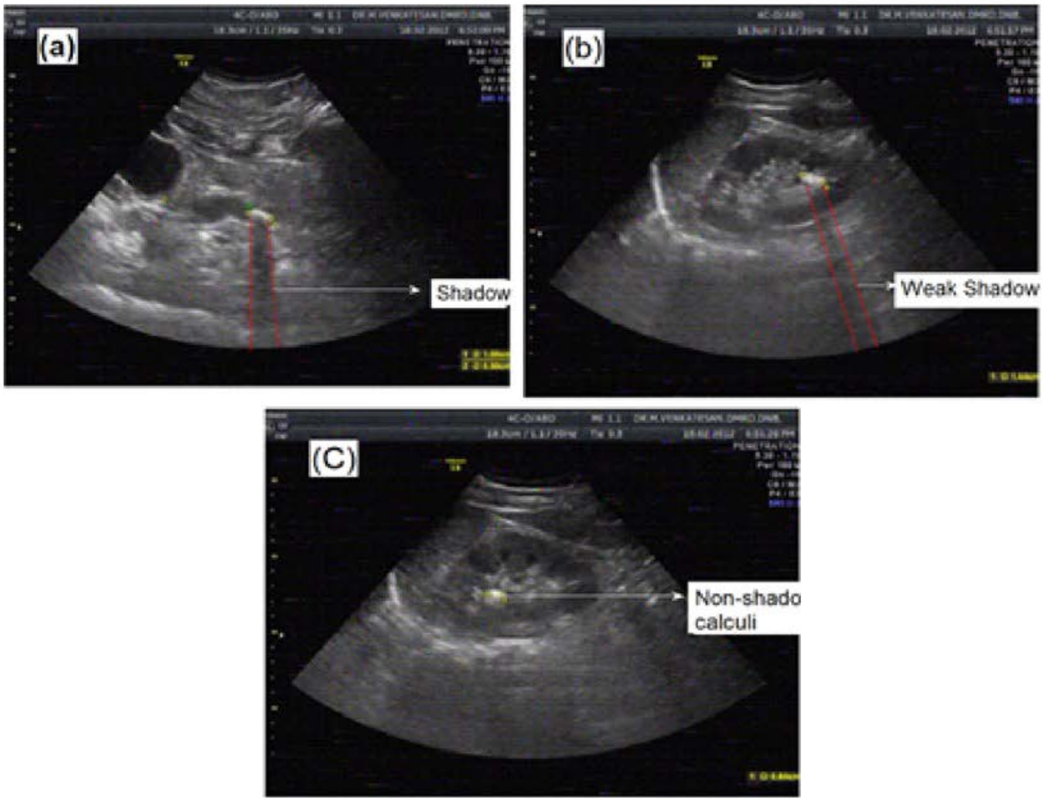

Fig. 1: Ultrasound imaging of renal calculi: a) Calculi with strong shadow; b) Calculi with weak shadow and c) Calculi with no shadow

Where:

μ_f = The mean

σ_f = The standard deviation of an reference noise free image f(x,y) over the selected window

μ_F = The mean

σ_F = The standard deviation of a despeckled image F(x,y) over the selected window

σ_{fF} = The co-variance between the original and despeckledimage over a window

Assume, $C_1 << \sigma_f, \sigma_F$ and $C_2 << \sigma_f, \sigma_F$:

$$C_1 = (K_1 L)^2 \tag{7}$$

Where:

$K_1 << 1$ = Small constant with default range [0.01 0.03]

L = The dynamic range of pixel value (default 255 for 8 bit gray scale images

$$C_1 = (k_1 L)^2 \tag{8}$$

$$C_3 = C_2 / 2 \tag{9}$$

Where:

$K_2 << 1$ = Small constant with default range [0.01 0.03]

C_1, C_2 = $C_3$are positive constants to nullify the effect of constants appearing in the SSIM Eq. 10

In ultrasound imaging, the edge preservation of original image is necessary while suppressing the noisesince the original image that often contains features of interest for therapeutic interpretation. The edge preserving index ($\beta\alpha$) used here is to determine the edge preserving capability of the filter:

$$\beta = \frac{r\left(\Delta f - \Delta\bar{f}, \Delta F - \Delta\bar{F}\right)}{\sqrt{r\left(\Delta f - \Delta\bar{f}, \Delta f - \Delta\bar{f}\right).r\left(\Delta F - \Delta\bar{F}, \Delta F - \Delta\bar{F}\right)}} \tag{10}$$

Where:

Δ = Laplacian operator

f = Original reference image and F is either the noise corrupted image or noise suppressed image

$\bar{f}$ and $\bar{F}$ = The means of f and F

This is a measure of correlation between two images. To perform this calculation the Laplacian operator is used in its 3×3 version.The Pratt's Figure of Merit (FOM) is an assessment criterion for edge detection process is given as:

$$\text{FOM} = \frac{1}{\max\left(N_d N_r\right)} \sum_{i=1}^{Nd} \frac{1}{1 + ad_i^2} \quad (11)$$

Where:

N_d = The number of pixels outlined by an automatic segmentation method

N_Y = The number of boundary pixels outlined by the experts

d_i^2 = The Euclidean distance between a boundary pixel outlined by the experts and the nearest boundary pixel extracted by automatic segmentation and a is a scaling constant (0.05 used here)

RESULTS AND DISCUSSION

It is easy to locate the renal calculi along with posterior acoustic shadowing. The posterior acoustic shadowing may be absent, weak or strong in various images based on its focal zone positioning as shown in Fig. 1. The shadowing can be strengthened by positioning the focal zone at the depth of the stone. However detection of calculi is difficult when stones are hidden by tissues that attenuates ultrasound beam such as renal sinus fat, mesenteric fat and bowel. In such cases the posterior acoustic shadowing may be weak or absent. The posterior acoustic shadowing also reduces the detection rate of calculi in the presence of multiple calculi one under another. Here the proposed algorithm is developed for calculi with no posterior acoustic shadow. The proposed stone detection algorithm tested qualitatively and quantitatively through experiments over ultrasound renal images acquired from various patients. The speckle noise is simulated in these images to do the experiment.

Figure 2 shows the speckle reduction performance of ABF, Lee filte (Nirali *et al.*, 2014) and wavelet thresholding (Wan and Supriyanto, 2010). Figure 2a is the ultrasound kidney image having a speckle noise of variance 0.1. Figure 2d shows that the ABF not only preserves the edges, but it also enhances the visual quality of the image comparatively with the other two filtering techniques shown in Fig. 2bc. In Fig. 2c, the clarity is poor than that of 2d but edge preservation is moderate. The kidney stone in Fig. 2d is difficult to interpret because of its blurred edges due to poor speckle reduction.

The values of FOM should be close to one for better edge detection performance of the algorithm presented. Here the value obtained is around 0.8 approximately, which indicates that, the ABF outperformed the other two filters. Figure 3a shows the graphical representation of Table 1. The ABF achieved better PSNR values than Lee filter and wavelet thresholding method.Higher the PSNR value indicates improvement in image quality due to noise minimization. Figure 3b gives the SSIM comparison between three filters represented in Table 2. The SSIM delivers more evidence about the image degradation of the denoised image. It can assess the similarity between the reference and denoised image better than PSNR.The SSIM value lies between 0 and 1. The value nearest to 0 indicates the bad quality of image whereas 1 for good quality.

The ABF algorithm for ultrasound denoising has better SSIM value than other two filters for different noise variance. It represents the visual quality of denoised output image is better with ABF. The β value should be close to 1 for optimal effect of edge preservation. The higher value of â indicates the effectiveness of the edge preservation capability as shown in Table 3 and Fig. 3c. It is evident that the wavelet thresholding technique has less β value when compared to Lee and ABF. Among them the ABF exhibits better performance in terms of edge preservationwhich is shown in Fig. 3c.

Table 1: Comparison of PSNR value for ABF, wavelet thresholding and lee filter obtainedfor different noise variances. The value for Fig. 3 is highlighted

Noise variance	Wavelet	Lee filter	ABF
σ = 0.5	27.5208	30.2506	66.8992
σ = 0.3	27.8132	30.7039	68.7900
σ = 0.1	30.1359	31.8694	73.0072
σ = 0.05	32.4883	32.8362	75.4035
σ = 0.03	34.2279	33.6719	76.9192
σ = 0.01	38.4170	35.5691	79.1743

Table 2: SSIM value for ABF, wavelet thresholding and Lee filter obtained different noise variances. The value for Fig. 3 is highlighted

Noise variance	Wavelet	Lee filter	ABF
σ = 0.5	0.5363	0.8268	0.9992
σ = 0.3	0.5928	0.8498	0.9994
σ = 0.1	0.8028	0.8976	0.9997
σ = 0.05	0.9146	0.9193	0.9998
σ = 0.03	0.9342	0.9321	0.9998
σ = 0.01	0.9651	0.9503	0.9999

Table 3: Comparison of edge preservation index (ß)for ABF, Wavelet thresholding and lee filter obtained for different noise variances. The value for Fig. 3 is highlighted

Noise variance	Wavelet	Lee filter	ABF
σ = 0.5	0.3445	0.4526	0.6641
σ = 0.3	0.2495	0.4521	0.6435
σ = 0.1	0.3879	0.5014	0.6872
σ = 0.05	0.3081	0.4873	0.5985
σ = 0.03	0.3882	0.5427	0.6388
σ = 0.01	0.2919	0.4139	0.5719

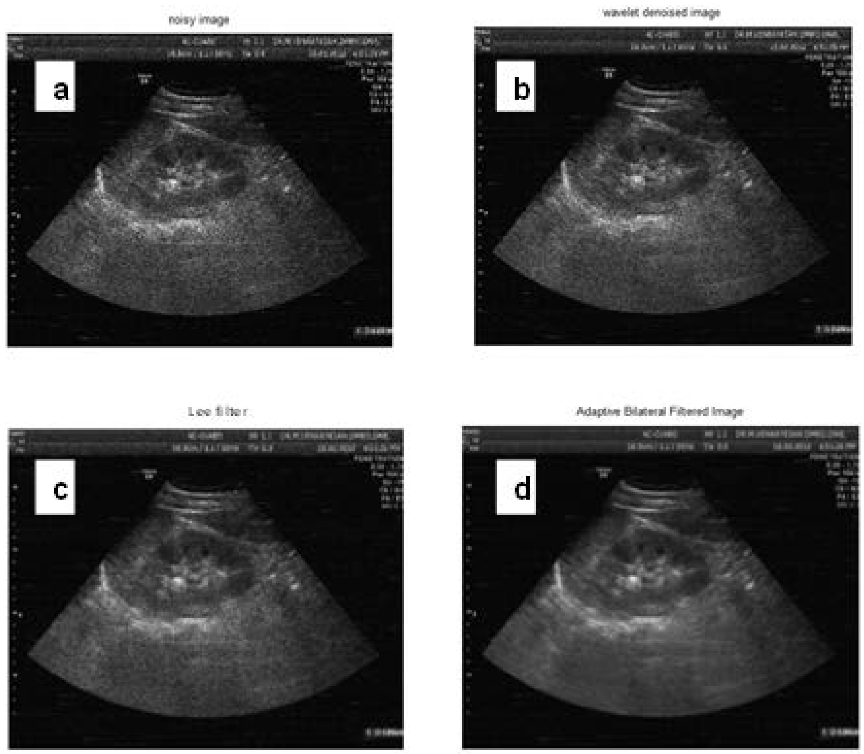

Fig. 2: Noise suppression performance: a) Noisy renal image; b) Wavelet thresholding and c) LEE filter and d) ABF

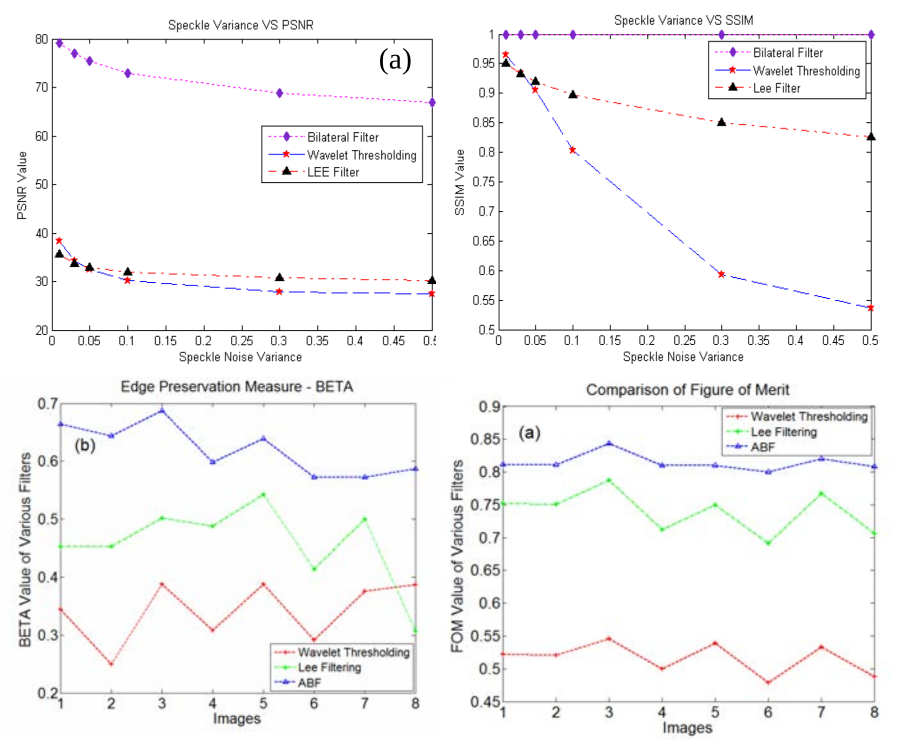

Fig. 3: a) Comparison of PSNR; b) Comparison of SSIM; c) Comparison of edge preservation index (ß) and d) Comparison of FOM

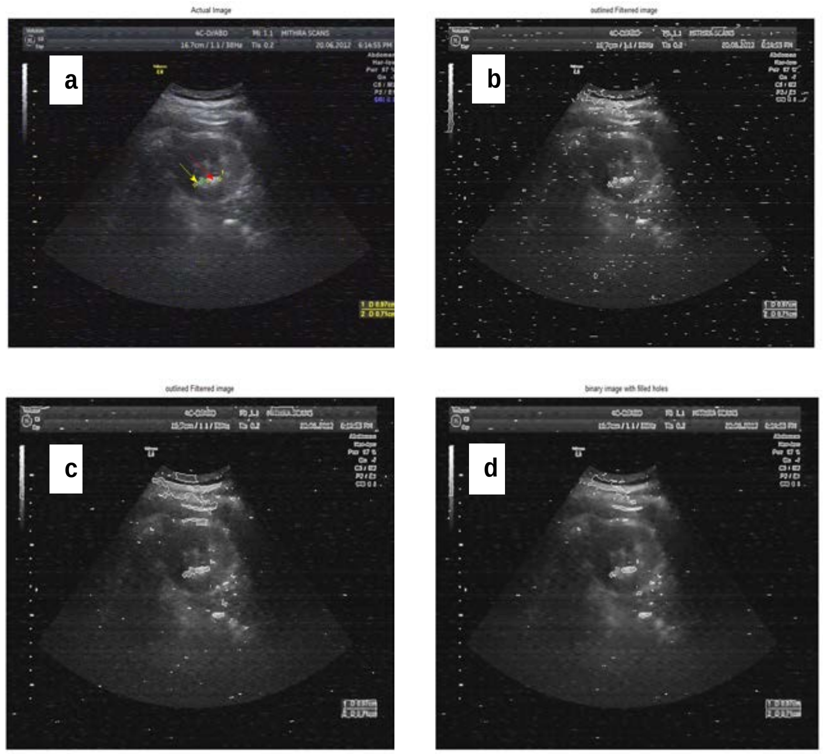

Fig. 4: Comparison of stone detection performance: a) Acquired original image with calculi region marked by expert; b) Stone detection with wavelet thresholding and morphological segmentation; c) Stone detection with lee filtering and morphological segmentation and d) Stone detection with ABF and morphological segmentation (Proposed method)

Table 4: Comparison of FOM for ABF, wavelet thresholding and lee filter obtained for different noise variances. The value for Fig. 5 is highlighted

Noise variance	Wavelet	Lee filter	ABF
$\sigma = 0.5$	0.5221	0.7527	0.8117
$\sigma = 0.3$	0.5208	0.7511	0.8111
$\sigma = 0.1$	0.5456	0.7877	0.8432
$\sigma = 0.05$	0.4999	0.7124	0.8099
$\sigma = 0.03$	0.5388	0.7497	0.8100
$\sigma = 0.01$	0.4789	0.6909	0.7998

For this analysis various images are considered with various noise variances. FOM of the proposed algorithm is calculated for a sample renal image for different value of noise variance is shown in Table 4 and Fig. 3d. The values of FOM should be close to one for better edge detection performance of the algorithm presented. Here the value obtained is around 0.8 approximately which indicates that, the ABF outperformed the other two filters.

Figure 4 shows the renal calculi detection performance of despeckled images using various filters. Figure 4a shows the ultrasound renal image with two calculi as an input reference image and the calculi present are marked by an expert. In wavelet filtered renal image, multiple segmented objects were detected which can lead to misinterpretation as shown in Fig. 4b. This is due the blurring of edges during the despecklingprocess. In the Lee filter image, instead of segmenting two different calculi, the segmentation process considers it in to a single calculus shown in Fig. 4c. Again this will leads to wrong diagnosis. Figure 4d shows the output of the proposed method where the exact segmentation is done. It proves that the ABF based morphological segmentation is more effective than any other method.

CONCLUSION

This study has presented a semi-automatic segmentation algorithm using adaptive bilateral filtering and morphological segmentation for medical ultrasound renal images. The performance of ABF is tested using PSNR, SSIM and edge preservation index for speckled ultrasound renal images. For comparison the Lee filter and wavelet thresholding techniques were considered. Morphological segmentation is also performed over filtered images. The effectiveness of morphological segmentation is tested using FOM. It shows that the segmentation through adaptive bilateral filtering is effective than other filters. The better noise reduction of ABF gives a trouble free analysis of renal images.

LIMITATIONS

The limitation of this method is the selection of optimal filter parameters. In this research a constant value of filter variances are assumed.

SUGGESTIONS

The future research will be the optimization of the ABF through the optimal selection of filter parameters according to the amount noise present.

ACKNOWLEDGEMENTS

The researchers would like to express their gratitude to Dr. P. Venkatesan, Mitra Scan, Salem for providing the necessary images for the analysis research.

REFERENCES

Balocco, S., C. Gatta, O. Pujol, J. Mauri and P. Radeva, 2010. SRBF: Speckle reducing bilateral filtering. Ultrasound Med. Biol., 36: 1353-1363.

Bhonsle, D., V. Chandra and G.R. Sinha, 2012. Medical image denoising using bilateral filter. Int. J. Image Graphics Signal Process., 4: 36-43.

Fwu, C.W., P.W. Eggers, P.L. Kimmel, J.W. Kusek and Z. Kirkali, 2013. Emergency department visits, use of imaging and drugs for urolithiasis have increased in the United States. Kidney Int., 83: 479-486.

Gupta A., B. Gosain and S. Kaushal, 2010. A comparison of two algorithms for automated stone detection in clinical B-mode ultrasound images of the abdomen. J. Clin. Monit. Comput., 24: 341-362.

Hafizah, W.M. and E. Supriyanto, 2012. Automatic generation of region of interest for kidney ultrasound images using texture analysis. Int. J. Biol. Biomed. Eng., 6: 26-34.

Hafizah, W.M., N.A. Tahir, E. Supriyanto, A. Arooj and S.M. Nooh, 2012. New technique towards operator independent kidney ultrasound scanning. Int. J. Comput., 6: 73-82.

Khan, A.N., M. Craig and J.A. Worrall, 2004. Sonographic mimics of renal calculi. J. Ultrasound Med., 23: 1361-1367.

Kop, A.M. and R. Hegadi, 2010. Kidney segmentation from ultrasound images using gradient vector force. IJCA. Spec. Issue Recent Trends Image Process. Pattern Recognit., 2010: 104-109.

Mitterberger, M., F. Aigner, L. Pallwein, G.M. Pinggera and R. Neururer et al., 2009. Sonographic detection of renal and ureteral stones: Value of the twinkling sign. Int. Braz. J. Urol., 35: 532-541.

Moe, O.W., 2006. Kidney stones: Pathophysiology and medical management. Lancet, 367: 333-344.

Nirali, S.H., S.J. Manasi, S.H. Dhrumil and K.S. Raviya, 2014. Analysis of renal calculi in ultrasound images using matlab. J. Inf. Knowl. Res. Electron. Commun. Eng., 3: 993-997.

Rafiei, H., F. Malekpoor, M. Amiri, M.M. Rahimi and H. Lalegani, 2014. Kidney stone development among older adults in Iran. J. Indian Acad. Geriatrics, 10: 10-13.

Raj, V.N.P. and T. Venkateswarlu, 2012. Ultrasound medical image denoising using hybrid bilateral filtering. Int. J. Comput. Appl., 56: 45-51.

Romero, V., H. Akpinar and D.G. Assimos, 2010. Kidney stones: A global picture of prevalence, incidence and associated risk factors. Rev. Urol., 12: e86-e96.

Santhiyakumari, N. and M. Madheswaran, 2008. Non-invasive evaluation of carotid artery wall thickness using improved dynamic programming technique. Signal Image Video Process., 2: 183-193.

Santhiyakumari, N., P. Rajendran and M. Madheswaran, 2011. Medical decision-making system of ultrasound carotid artery intima-media thickness using neural networks. J. Digital Imaging, 24: 1112-1125.

Shi, W., J. Li and M. Wu, 2010. An image denoising method based on multiscale wavelet thresholding and bilateral filtering. Wuhan Univ. J. Nat. Sci., 15: 148-152.

Sridhar, S., 2012. Segmentation of ureteric and bladder calculi in ultrasound images. J. Comput. Sci., 8: 716-720.

Tamilselvi, M.P. and D.P. Thangaraj, 2011. Computer aided diagnosis system for stone detection and early detection of kidney stones. J. Comput. Sci., 7: 250-254.

Tamilselvi, M.P. and P. Thangaraj, 2010. Segmentation of renal calculi from ultrasound images. J. Comput. Appl., 3: 36-40.

Tamilselvi, P.R. and P. Thangaraj, 2011. An efficient segmentation of calculi from US renal calculi images using ANFIS system. Eur. J. Sci. Res., 55: 323-333.

Tamilselvi, P.R. and P. Thangaraj, 2012. Segmentation of calculi from ultrasound kidney images by region indictor with contour segmentation method. Global J. Comput. Sci. Technol., 11: 43-51.

Tamiselvi, P.R., 2013. Detection of renal calculi using semi automatic segmentation approach. Int. J. Eng. Sci. Innov. Technol., 2: 547-552.

Tang, J., S. Guo, Q. Sun, Y. Deng and D. Zhou, 2010. Speckle reducing bilateral filter for cattle follicle segmentation. BMC. Genomics, 11: S2-S9.

Tomasi, C. and R. Manduchi, 1998. Bilateral filtering for gray and color images. Proceedings of the 6th International Conference on Computer Vision, January 4-7, 1998, Bombay, India, pp: 839-846.

Wan, M.H. and E. Supriyanto, 2011. Comparative evaluation of ultrasound kidney image enhancement techniques. Int. J. Comput. Appl., 21: 15-19.

Zayid, A.R.A., N.M. Ali and A. Ahuja, 2014. Study on prevalence and management of renal stones among Omani in-patients at Sohar Hospital. Scholars J. Appl. Med. Sci., 2: 22-33.